

1 **Mass spectrometric measurement of hydrogen isotope fractionation for the**  
2 **reactions of chloromethane with OH and Cl**

3

4 **Frank Keppler<sup>1,2,3</sup>, Enno Bahlmann<sup>4,5</sup>, Markus Greule<sup>1,3</sup>, Heinz Friedrich Schöler<sup>1</sup>**  
5 **Julian Wittmer<sup>6,7</sup> and Cornelius Zetzsch<sup>3,6</sup>**

6 [1] Institute of Earth Sciences, Heidelberg University, Im Neuenheimer Feld 234-236, 69120  
7 Heidelberg, Germany

8 [2] Heidelberg Center for the Environment (HCE), Heidelberg University, D-69120  
9 Heidelberg, Germany

10 [3] Max-Planck-Institute for Chemistry, Hahn-Meitner-Weg 1, 55128 Mainz, Germany

11 [4] Leibniz Centre for Tropical Marine Research, Fahrenheitstraße 6, 28359 Bremen

12 [5] Institute of Geology, University Hamburg, Bundesstrasse 55, 20146 Hamburg, Germany

13 [6] Atmospheric Chemistry Research Unit, BayCEER, University of Bayreuth, Dr Hans-  
14 Frisch Strasse 1–3, D-95448 Bayreuth, Germany.

15 [7] Agilent Technologies Sales & Services GmbH & Co. KG, Hewlett-Packard-Str. 8, 76337  
16 Waldbronn, Germany

17 Correspondence to: Frank Keppler ([frank.keppler@geow.uni-heidelberg.de](mailto:frank.keppler@geow.uni-heidelberg.de))

18

19 **Abstract**

20 Chloromethane (CH<sub>3</sub>Cl) is an important provider of chlorine to the stratosphere but detailed  
21 knowledge of its budget is missing. Stable isotope analysis is potentially a powerful tool to  
22 constrain CH<sub>3</sub>Cl flux estimates. The largest degree of isotope fractionation is expected to  
23 occur for deuterium in CH<sub>3</sub>Cl in the hydrogen abstraction reactions with its main sink  
24 reactant tropospheric OH and its minor sink reactant Cl atoms. We determined the isotope  
25 fractionation by stable hydrogen isotope analysis of the fraction of CH<sub>3</sub>Cl remaining after  
26 reaction with hydroxyl and chlorine radicals in a 3.5 m<sup>3</sup> Teflon smog-chamber at 293 ± 1K.  
27 We measured the stable hydrogen isotope values of the unreacted CH<sub>3</sub>Cl using compound  
28 specific thermal conversion isotope ratio mass spectrometry. The isotope fractionations of  
29 CH<sub>3</sub>Cl for the reactions with hydroxyl and chlorine radicals were found to be -264 ± 45 ‰  
30 and -280 ± 11 ‰, respectively. For comparison, we performed similar experiments using

31 methane (CH<sub>4</sub>) as the target compound with OH and obtained a fractionation constant of -205  
32 ± 6 ‰ which is in good agreement with values previously reported. The observed large  
33 kinetic isotope effects are helpful when employing isotopic analyses of CH<sub>3</sub>Cl in the  
34 atmosphere to improve our knowledge of its atmospheric budget.

35

## 36 **1 Introduction**

37 Chloromethane (often called methyl chloride) is the most abundant chlorine containing trace  
38 gas in the Earth's atmosphere, currently with a global mean mixing ratio of ~540 ± 5 parts  
39 per trillion by volume (pptv) and an atmospheric lifetime of 1.0–1.2 years (Carpenter et al.,  
40 2014). The global emissions of CH<sub>3</sub>Cl have been estimated to be in the range of 4 to 5 Tg yr<sup>-1</sup>  
41 (1 Tg = 10<sup>12</sup> g) stemming from predominantly natural but also anthropogenic sources  
42 (Montzka and Fraser, 2003; WMO, 2011; Carpenter et al., 2014). However, current estimates  
43 of the CH<sub>3</sub>Cl global budget and the apportionment between sources and sinks are still highly  
44 uncertain. Known natural sources of CH<sub>3</sub>Cl include tropical plants (Yokouchi et al., 2002;  
45 Yokouchi et al., 2007; Umezawa et al., 2015), wood-rotting fungi (Harper, 1985), oceans  
46 (Moore et al., 1996, Kolusu et al. 2017), plants of salt marshes (Rhew et al., 2003; Rhew et  
47 al., 2000), aerated and flooded soil (Redeker et al., 2000; Keppler et al., 2000), senescent  
48 leaves and leaf litter (Hamilton et al., 2003; Derendorp et al., 2011) and wild fires.  
49 Anthropogenic CH<sub>3</sub>Cl release to the atmosphere comes from the combustion of coal and  
50 biomass with minor emissions from cattle (Williams et al., 1999) and humans (Keppler et al.,  
51 2017). In addition, it has been reported that emissions from industrial sources, particularly in  
52 China, might be much higher than previously assumed (Li et al., 2016).

53 The dominant sink for atmospheric CH<sub>3</sub>Cl results from the reaction with photochemically-  
54 produced hydroxyl radicals (OH), currently estimated at about 2.8 Tg yr<sup>-1</sup> (Carpenter et al.,  
55 2014). Furthermore, in the marine boundary layer the reaction of CH<sub>3</sub>Cl with chlorine  
56 radicals (Cl) represents another sink estimated to account for up to 0.4 Tg yr<sup>-1</sup> (Khalil et al.,  
57 1999; Montzka and Fraser, 2003). Microbial CH<sub>3</sub>Cl degradation in soils may be a relevant  
58 additional global sink (McAnulla et al., 2001; Harper et al., 2003; Miller et al., 2004; Jaeger  
59 et al., 2018a) but its impact on the global CH<sub>3</sub>Cl budget is still highly uncertain. The  
60 microbial CH<sub>3</sub>Cl soil sink strength has been estimated to range from 0.1 to 1.6 Tg yr<sup>-1</sup>  
61 (Harper et al., 2003; Keppler et al., 2005; Carpenter et al., 2014). Moreover, small  
62 proportions of tropospheric CH<sub>3</sub>Cl are lost to the stratosphere (146 Gg yr<sup>-1</sup>, 1 Gg = 10<sup>9</sup> g) and  
63 to cold polar oceans (370 Gg yr<sup>-1</sup>) though oceans in total are a net source (Carpenter et al.,

64 2014). Loss of tropospheric CH<sub>3</sub>Cl to the stratosphere is a result of turbulent mixing and the  
65 transport process itself is not thought to cause a substantial isotope fractionation (Thompson  
66 et al. 2002).

67 A potentially powerful tool in the investigation of the budgets of atmospheric volatile organic  
68 compounds is the use of stable isotope ratios (Brenninkmeijer et al., 2003; Gensch et al.,  
69 2014). The general approach is that the atmospheric isotope ratio of a compound (e.g. CH<sub>3</sub>Cl)  
70 is considered to equal the sum of isotopic fluxes from all sources corrected for kinetic  
71 isotopic fractionations that happen in sink processes:

$$72 \quad \delta^2 H^{atm} = \sum_{i=1}^n \Phi_i^{source} \times \delta^2 H_i^{source} + \sum_{j=1}^n \Phi_j^{sink} \times \epsilon_j^{sink} \quad (1)$$

73 where  $\delta^2 H^{atm}$  and  $\delta^2 H_i^{source}$  are the hydrogen isotope values of CH<sub>3</sub>Cl in the atmosphere and  
74 of the different sources i in per mil.  $\Phi_i$  and  $\Phi_j$  are the CH<sub>3</sub>Cl flux fraction for each source and  
75 sink.  $\epsilon_j$  is the isotope fractionation of each sink j in per mil.

76 The isotopic composition of atmospheric compounds might be altered by the kinetic isotope  
77 effects of physical, chemical or biological loss processes. The kinetic isotope effect (KIE) is  
78 usually defined as:

$$79 \quad KIE = \frac{k_1}{k_2} \quad (2)$$

80 where  $k_1$  and  $k_2$  are the reaction rate constants for loss of the lighter and the heavier  
81 isotopologues, respectively. The KIE is typically expressed as isotope fractionation  $\epsilon$  (also  
82 termed isotope enrichment constant) or isotope fractionation constant  $\alpha$ .

83 First approaches of an isotope mass balance regarding stable carbon isotopes of CH<sub>3</sub>Cl have  
84 been provided by Keppler et al. (2005) and Saito & Yokouchi (2008). Several studies have  
85 investigated the stable carbon isotope source signature of CH<sub>3</sub>Cl produced via biotic and  
86 abiotic processes, however, for a more detailed overview we refer readers to the studies of  
87 Keppler et al. (2005) and Saito & Yokouchi (2008). Moreover, researchers have measured the  
88 KIE of stable carbon isotopes of CH<sub>3</sub>Cl during oxidation or biodegradation by bacterial  
89 isolates (Miller et al., 2001; Nadalig et al., 2013; Nadalig et al., 2014) or in soils under  
90 laboratory conditions (Miller et al., 2004; Jaeger et al., 2018a). The first, and so far, only  
91 available analysis of the KIE for reaction of CH<sub>3</sub>Cl with OH has been reported by Gola et al.

92 (2005) and this revealed an unexpectedly large stable carbon isotope fractionation. The  
93 experiments were carried out in a smog chamber using long path Fourier-transform infrared  
94 spectroscopy (FTIR) detection. However, we consider it important to confirm this result  
95 using another measurement technique such as stable isotope ratio mass spectrometry (IRMS).

96 So far most isotopic investigations of CH<sub>3</sub>Cl have focused on stable carbon isotope  
97 measurements but stable hydrogen isotope measurements including both sources and sinks of  
98 CH<sub>3</sub>Cl have also recently become available (Greule et al., 2012; Nadalig et al., 2014; Nadalig  
99 et al., 2013; Jaeger et al., 2018b; Jaeger et al., 2018a). Moreover, relative rate experiments  
100 have been carried out for three isotopologues of CH<sub>3</sub>Cl and their reactions with Cl and OH.  
101 The OH and Cl reaction rates of CH<sub>2</sub>DCl were measured by long-path FTIR spectroscopy  
102 relative to CH<sub>3</sub>Cl at 298 ± 2 K and 1 atm (Sellevåg et al., 2006) (Table 1).

103 In this manuscript, using a 3.5 m<sup>3</sup> Teflon smog chamber and IRMS measurements, we  
104 present results from kinetic studies of the hydrogen isotope fractionation in the atmospheric  
105 OH and Cl loss processes of CH<sub>3</sub>Cl. Furthermore, we also measured the isotope fractionation  
106 for the reaction between methane (CH<sub>4</sub>) and OH using a similar experimental design and  
107 compared this value with those from previous studies.

## 108 **2 Materials and Methods**

### 109 **2.1 Smog chamber experiments with chloromethane**

110 The isotope fractionation experiments were performed in a 3.5 m<sup>3</sup> Teflon smog-chamber  
111 (fluorinated ethylene propylene, FEP 200A, DuPont, Wilmington, DE, USA) with initial  
112 CH<sub>3</sub>Cl mixing ratio of 5 to 10 parts per million by volume (ppmv). Atomic chlorine were  
113 generated via photolysis of molecular chlorine (Cl<sub>2</sub>) (Rießner Gase, 0.971% Cl<sub>2</sub> in N<sub>2</sub>) by a  
114 solar simulator with an actinic flux comparable to the sun in mid-summer in Germany  
115 (Bleicher et al., 2014). Hydroxyl radicals were generated via the photolysis of ozone (O<sub>3</sub>) at  
116 253.7 nm in the presence of water vapor (RH = 70%) (produced by double-distilled water in a  
117 three-neck bottle humidifier) and/or H<sub>2</sub>. To obtain efficient OH formation, a Philips TUV  
118 lamp T8 (55 W) was welded in Teflon film (FEP 200) and mounted inside the smog chamber.  
119 O<sub>3</sub> was monitored by a chemiluminescence analyzer (UPK 8001). The chamber was  
120 continuously flushed with purified, hydrocarbon-free zero air (zero-air-generator, cmc  
121 instruments, <1 ppbv of O<sub>3</sub>, <500 pptv NO<sub>x</sub>, <100 ppbv of CH<sub>4</sub>) at a rate of 4 L min<sup>-1</sup> to  
122 maintain a slight overpressure of 0.5-1 Pa logged with a differential pressure sensor  
123 (Kalinsky Elektronik DS1). The quality of the air inside the chamber in terms of possible

124 contamination was controlled by monitoring NO and NO<sub>x</sub> (EcoPhysics CLD 88p, coupled  
125 with a photolytic converter, EcoPhysics PLC 860). Perfluorohexane (PFH) with an initial  
126 mixing ratio of ~25 parts per billion by volume (ppbv) was used as an internal standard to  
127 correct the resulting concentrations for dilution. The temperature was set to 20±1°C and  
128 monitored, together with the relative humidity, by a Teflon-cased sensor (Rotronic, HC2-  
129 IC102). To guarantee constant mixing and small temperature gradients, a Teflon fan was  
130 mounted and operated inside the chamber. More detailed specification of the smog chamber  
131 can be found elsewhere (e.g. Wittmer et al., 2015). The mixing ratios of CH<sub>3</sub>Cl and PFH  
132 were quantified by a Hewlett Packard HP 6890 gas chromatograph coupled to a MSD 5973  
133 mass spectrometer (GC-MS, Agilent Technologies, Palo Alto, CA) with a time resolution of  
134 15 minutes throughout the experiments. Two CH<sub>3</sub>Cl reference gases from Linde (1006±12  
135 ppmv diluted in N<sub>2</sub>) and Scott (1 ppmv) were used for calibration. The abundance of CH<sub>3</sub>Cl  
136 relative to PFH was used to calculate the remaining fraction of CH<sub>3</sub>Cl (equation 4). The  
137 relative standard deviation of this procedure was determined prior to each experiment and  
138 also during control experiment and ranged between 1.3 and 1.9%. Aliquots (5 ml) were  
139 withdrawn from the chamber with a gas tight syringe, injected into a stream of He (30 ml  
140 min<sup>-1</sup>) and directed to a pre-concentration unit that was attached to the GC-MS. The pre-  
141 concentration unit consisted of a simple 8 port valve (VICI Valco) equipped with two  
142 cryotrap made of fused silica, which were immersed in liquid nitrogen for trapping the  
143 analytes. Prior to each sample measurement, a gaseous standard (5 ml of 100 ppmv CH<sub>3</sub>Cl in  
144 N<sub>2</sub>) was measured. Figure 1 shows the design of the smog chamber used in our experiments.

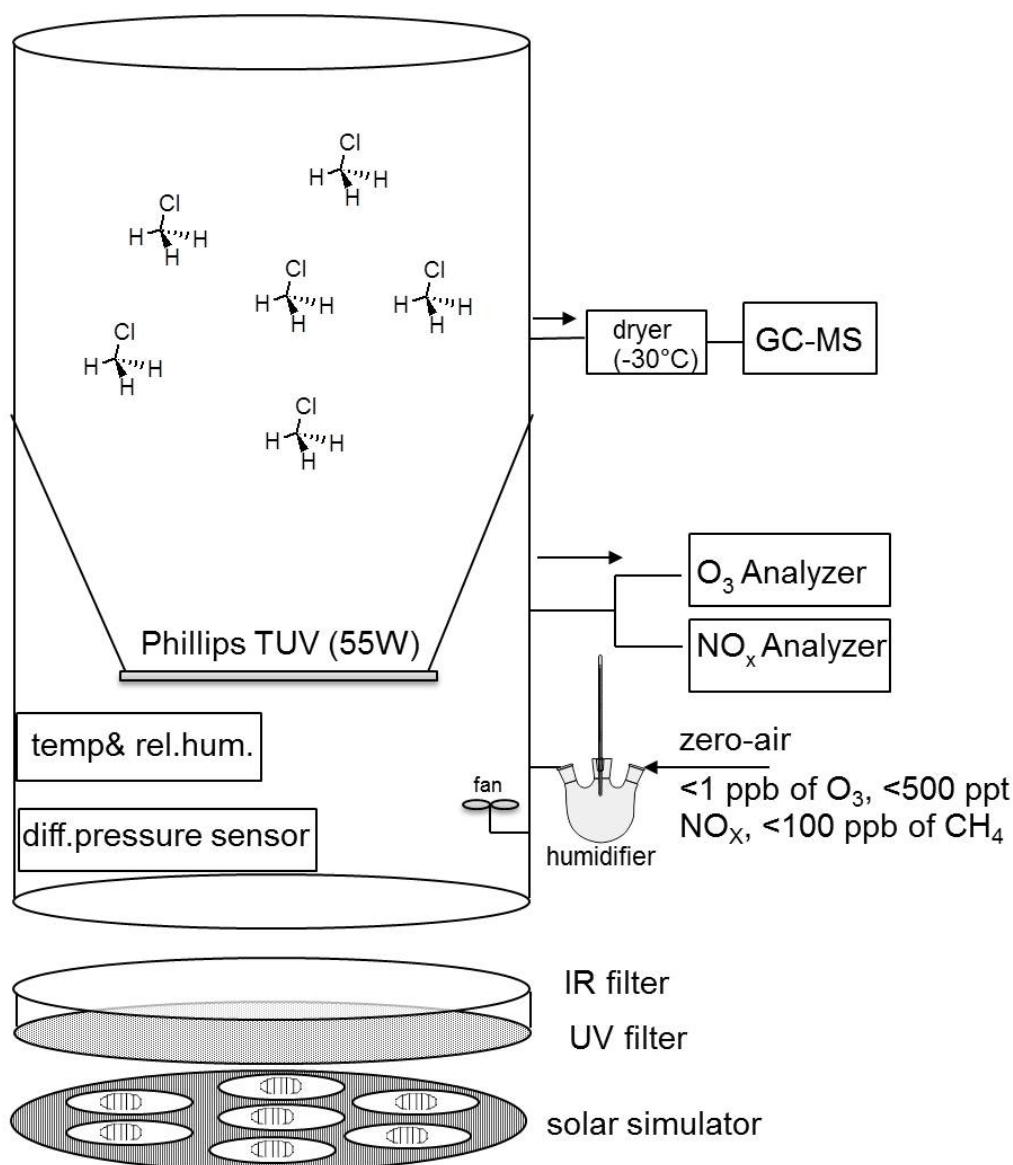
145 In the CH<sub>3</sub>Cl and OH experiments (1 to 3) 2000 ppmv H<sub>2</sub> was used to scavenge chlorine  
146 atoms originating from the photolysis or oxidation of formyl chloride (HCOCl), which forms  
147 as an intermediate in the reaction cascade. Under the experimental conditions typically more  
148 than 70% of the CH<sub>3</sub>Cl was degraded within 6 to 10 h. From each experiment (CH<sub>3</sub>Cl + OH  
149 and CH<sub>3</sub>Cl + Cl) 10 to 15 canister samples (2 L stainless steel, evacuated <10<sup>-4</sup> mbar) were  
150 collected at regular time intervals for subsequent stable hydrogen isotope measurements at  
151 Heidelberg University. An overview of the experimental details (Table S1) and control  
152 measurements is provided in the Supplementary.

153

154

155

156 **Figure 1:** Scheme of the experimental smog chamber



157

158

159

## 160 **2.2 Smog chamber degradation experiments with methane**

161 The  $\text{CH}_4$  degradation experiments were carried under the same conditions as the  $\text{CH}_3\text{Cl}$   
162 degradation experiments but without PFH as an internal standard. Instead we used the  
163 flushing flow rate of zero air to account for the dilution during the experiment. The initial  
164  $\text{CH}_4$  mixing ratio was 6 ppmv. Throughout these experiments  $\text{CH}_4$  and  $\text{CO}_2$  mixing ratios  
165 were monitored with a Picarro G225i cavity ring down spectrometer directly connected to the  
166 chamber. For more details see information provided in the Supplementary.

167

## 168 2.3 Stable hydrogen isotope analysis using isotope ratio mass spectrometry

### 169 2.3.1 Chloromethane

170 Stable hydrogen isotope ratios of CH<sub>3</sub>Cl were measured by an in-house built cryogenic pre-  
171 concentration unit coupled to a Hewlett Packard HP 6890 gas chromatograph (Agilent  
172 Technologies, Palo Alto, CA) and an isotope ratio mass spectrometer (IRMS) (Isoprime,  
173 Manchester, UK) as described in detail by Greule et al. (2012). Diverging from the method of  
174 Greule et al. (2012) a ceramic tube reactor without chromium pellets at 1450°C was instead  
175 used for high-temperature conversion (HTC). A tank of high-purity H<sub>2</sub> (Alphagaz 2,  
176 hydrogen 6.0, Air Liquide, Düsseldorf, Germany) with a δ<sup>2</sup>H value of ~-250 ‰ versus  
177 VSMOW was used as the working gas. The conventional delta notation, expressing the  
178 isotopic composition of the sample relative to that of VSMOW standard (Vienna Standard  
179 Mean Ocean Water) in per mil is used. All sample δ<sup>2</sup>H values were measured relative to an  
180 in-house working standard of known δ<sup>2</sup>H value. The CH<sub>3</sub>Cl working standard was calibrated  
181 against IAEA standards VSMOW and SLAP using TC/EA-IRMS (elemental analyser-  
182 isotopic ratio mass spectrometer, IsoLab, Max Planck Institute for Biogeochemistry, Jena,  
183 Germany) resulting in a δ<sup>2</sup>H value of  $-140.1 \pm 1.0$  ‰ vs. VSMOW (n = 10, 1σ). The H<sub>3</sub><sup>+</sup>  
184 factor, determined daily during this investigation (two different measurement periods), was in  
185 the range of 5.75 - 6.16 (first period) and 8.90 - 9.21 (second period). The mean precision  
186 based on replicate measurements (n = 6) of the CH<sub>3</sub>Cl working standard was 2.1 and 3.8 ‰  
187 for the first and second measurement periods, respectively. Samples were analyzed three  
188 times (n = 3), and the standard deviations (SD) of the measurements were in the range of 1.2  
189 to 103.8 ‰. Lowest SD were observed for samples with lowest δ<sup>2</sup>H values (~-140 ‰) and  
190 highest mixing ratios and higher SD for samples with highest δ<sup>2</sup>H values (~+800 ‰) and  
191 lowest mixing ratios.

192 Please note that the above described 1-point calibration of the δ<sup>2</sup>H data might be affected by  
193 an additional error ("scale compression") and particularly might affect the uncertainties of the  
194 very positive δ<sup>2</sup>H values. Unfortunately CH<sub>3</sub>Cl working standards with distinct isotopic  
195 signatures spanning the full range of measured δ<sup>2</sup>H values (-150 to ~+800 ‰) are not  
196 currently available to eliminate or minimize such an error.

197

198

199

### 200 2.3.2 Methane

201 Stable hydrogen isotope ratios of CH<sub>4</sub> were analyzed using an in-house built cryogenic pre-  
202 concentration unit coupled to a Hewlett Packard HP 6890 gas chromatograph (Agilent  
203 Technologies, Palo Alto, CA) and an isotope ratio mass spectrometer (DeltaPlus XL,  
204 ThermoQuest Finnigan, Bremen, Germany). The working gas was the same as that used for  
205 δ<sup>2</sup>H analysis of CH<sub>3</sub>Cl (c.f. section 2.3.1.).

206 All δ<sup>2</sup>H values obtained from analysis of CH<sub>4</sub> were corrected using two CH<sub>4</sub> working  
207 standards (isometric instruments, Victoria, Canada) calibrated against IAEA and NIST  
208 reference substances (not specified by the company). The calibrated δ<sup>2</sup>H values of the  
209 working standard in ‰ vs. V-SMOW were -144 ± 4 ‰ and -138 ± 4 ‰.

210 The H<sub>3</sub><sup>+</sup> factor determined daily during the two week measurement period was in the range  
211 2.38–2.43. The daily average precision based on replicate measurements of the CH<sub>4</sub> working  
212 standard was 4.9 ‰ (n = 7). Samples were analyzed 3 times (n = 3), and the SD of the  
213 measurements were in the range of 1.4 to 40.9 ‰. Lowest SD were observed for samples  
214 with lowest δ<sup>2</sup>H values (~-140 ‰) and highest mixing ratios and higher SD for samples with  
215 highest δ<sup>2</sup>H values (~+800 ‰) and lowest mixing ratios.

216

### 217 2.4 Kinetic isotope effect, fractionation constant α and the isotope enrichment constant ε

218 In this study the isotope fractionation constant α and the isotope enrichment constant ε are  
219 derived from the slope of the Rayleigh plot according to (Clark and Fritz, 1997; Elsner et al.,  
220 2005) and equation 2:

221

$$222 \ln \frac{R_t}{R_0} = \left( \frac{\delta^{2H}_t + 1}{\delta^{2H}_0 + 1} \right) = \ln \frac{(\delta^{2H}_0 + \Delta\delta^{2H} + 1)}{(\delta^{2H}_0 + 1)} \cong (\alpha - 1) \cdot \ln f = \varepsilon \cdot \ln f \quad (3)$$

223

224 Where  $R_t$  and  $R_0$  are the <sup>2</sup>H/<sup>1</sup>H ratios in CH<sub>3</sub>Cl or CH<sub>4</sub> at the different time points and time  
225 zero, respectively, and  $f$  is the remaining CH<sub>3</sub>Cl or CH<sub>4</sub> fraction at the different time points.  
226 Negative values of ε indicates that the remaining CH<sub>3</sub>Cl or CH<sub>4</sub> is enriched in the heavier  
227 isotope and corresponds to a α < 1, meaning that over the entire experiment, the heavier  
228 CH<sub>2</sub>DCl or CHD react by this factor more slowly than the lighter CH<sub>3</sub>Cl or CH<sub>4</sub>.

229 The kinetic isotope effect is then calculated as:

230 
$$KIE = \frac{1}{\alpha} \tag{4}$$

231 To correct for ongoing analyte dilution the remaining fraction  $f$  has been calculated as follows

232 
$$f = c_{xT} * c_{i0} / (c_{x0} * c_{iT}) \tag{5}$$

233 where  $c_{x0}$  and  $c_{xT}$  are the mixing ratios of CH<sub>3</sub>Cl at time zero and time t and  $c_{i0}$  and  $c_{iT}$  are the  
234 respective concentrations of the internal standard PFH.

235

### 236 **3 Results**

237 Three experiments of CH<sub>3</sub>Cl degradation with OH were performed between 25/02/2014 and  
238 the 03/02/2015. Under the experimental conditions (see methods section and Supplementary)  
239 more than 70% of the CH<sub>3</sub>Cl was degraded within 6 to 10 h. The results from these  
240 experiments are shown in Figure 2. Both the trend of changes in  $\delta^2\text{H}$  values of CH<sub>3</sub>Cl as well  
241 as the remaining fraction of CH<sub>3</sub>Cl observed in the three independent experiments are in good  
242 agreement (Figure 2a). The calculated  $\epsilon$  values for experiments 1 to 3 are  $-264 \pm 7 \text{ ‰}$ ,  $-219 \pm$   
243  $6 \text{ ‰}$  and  $-308 \pm 8 \text{ ‰}$  respectively (Figure 2b), with a correlation coefficient  $R^2$  of the slope  
244 of the regression line of 0.99 for all three experiments.

245

246 **Figure 2:** Reaction of CH<sub>3</sub>Cl and OH. Three independent experiments (triangles, dots and  
247 squares) were carried out using an initial mixing ratio of 5 to 10 ppmv CH<sub>3</sub>Cl. More than  
248 70% of the CH<sub>3</sub>Cl was degraded within 6 to 10 h. (a) Measured  $\delta^2\text{H}$  values (filled circles,  
249 triangles and squares) of CH<sub>3</sub>Cl versus residual fraction (open circles, triangles and squares)  
250 of CH<sub>3</sub>Cl (calculated from changes of CH<sub>3</sub>Cl and PFH). Error bars of  $\delta^2\text{H}$  value of CH<sub>3</sub>Cl  
251 indicate the standard deviation (SD) of the mean of three replicate measurements. Some error  
252 bars lie within the symbol. (b) Rayleigh plot (equation 2). Error bars were calculated by error  
253 propagation including uncertainties in  $\delta^2\text{H}$  values of CH<sub>3</sub>Cl and the remaining fraction.  
254 Dashed lines represent 95% confidence intervals of the linear regressions (bold lines).

255

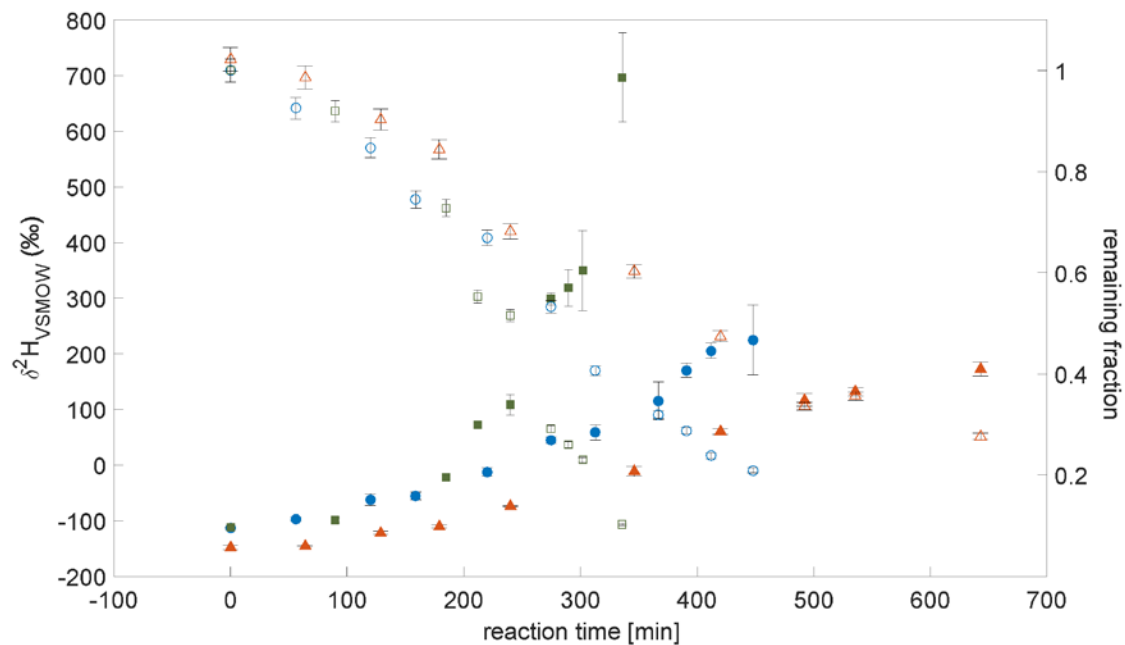
256

257

258

259

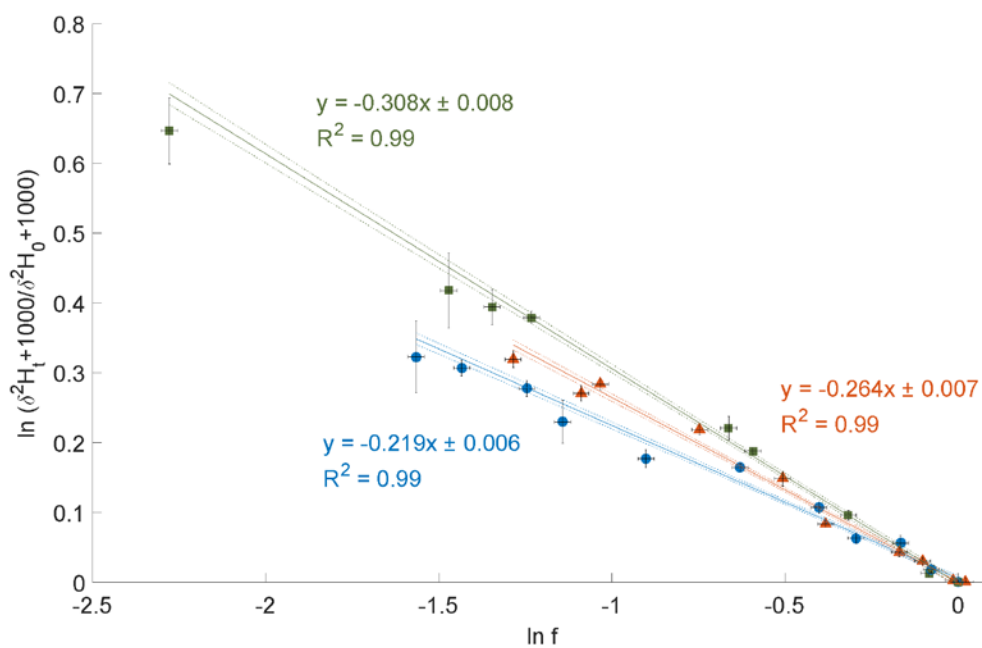
2a)



260

261

2b)



262

263

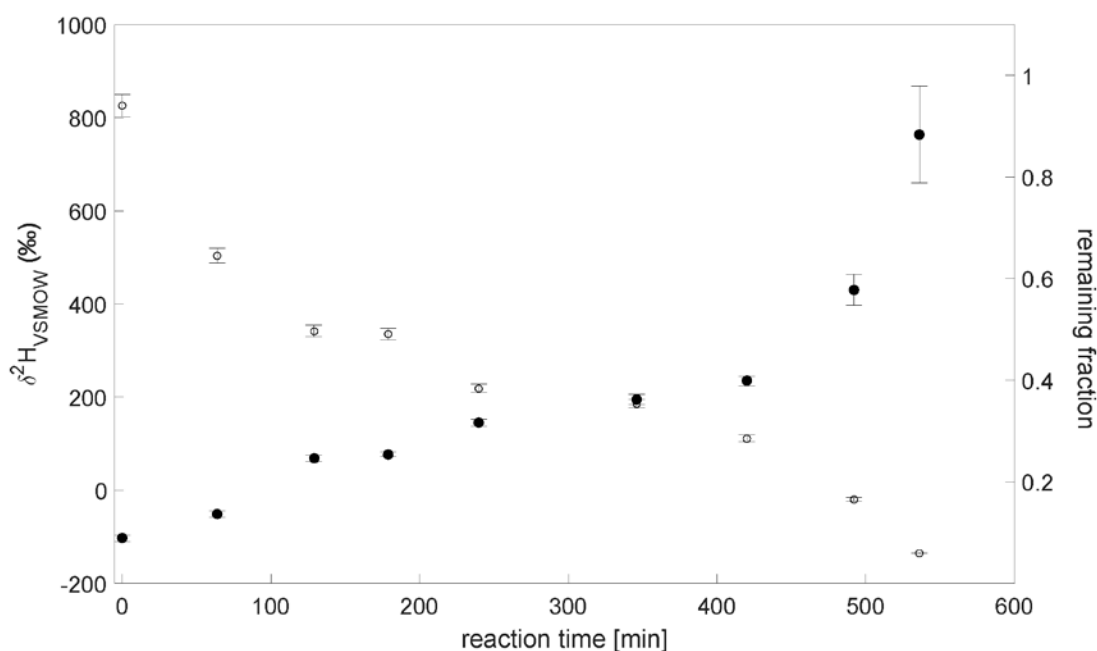
264 The  $\text{CH}_3\text{Cl}$  degradation with Cl experiment was conducted on the 18/02/2014. Here, over  
265 90% of  $\text{CH}_3\text{Cl}$  was degraded during reaction with Cl radicals within 7 to 8 hours (Figure 3a).

266 The calculated  $\varepsilon$  of experiment 3 is  $-280 \pm 11$  ‰ (Figure 3b) with a correlation coefficient of  
267 the slope of the regression line of 0.99. Due to limited analytical resources it was not  
268 possible to repeat this experiment.

269

270 **Figure 3:** Reaction of  $\text{CH}_3\text{Cl}$  and  $\text{Cl}$ . Initial mixing ratio of  $\text{CH}_3\text{Cl}$  was  $\sim 10$  ppmv. More than  
271 90% of the  $\text{CH}_3\text{Cl}$  was degraded within 7 to 8 h. (a) Measured  $\delta^2\text{H}$  values (filled circles) of  
272  $\text{CH}_3\text{Cl}$  versus residual fraction (open diamonds)  $\text{CH}_3\text{Cl}$ . Error bars of  $\delta^2\text{H}$  values of  $\text{CH}_3\text{Cl}$   
273 indicate the standard deviation (SD) of the mean of three replicate measurements. Some error  
274 bars lie within the symbol. (b) Rayleigh plot (equation 2). Data are expressed as the  
275 mean  $\pm$  standard error of the mean,  $n=3$ . Error bars were calculated by error propagation  
276 including uncertainties in  $\delta^2\text{H}$  values of  $\text{CH}_3\text{Cl}$ . Dashed lines represent 95% confidence  
277 intervals of the linear regressions (bold line).

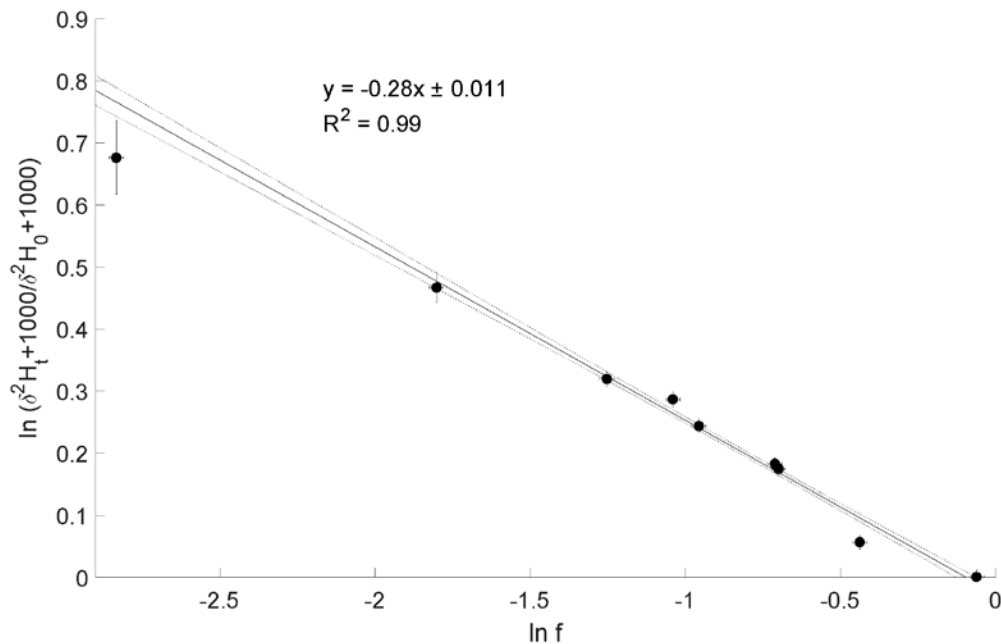
3a)



278

279

3b



280

281

282 The experiment to determine the isotope enrichment constant of the degradation of CH<sub>4</sub> by  
 283 hydroxyl radicals was conducted on the 02/02/2015. Over 80% of CH<sub>4</sub> was degraded during  
 284 reaction with OH radicals within 7 hours (Figure 4a). The calculated  $\epsilon$  of experiment 4 is -  
 285  $205 \pm 6$  ‰ (Figure 4b) with a correlation coefficient of the slope of the regression line of  
 286 0.99.

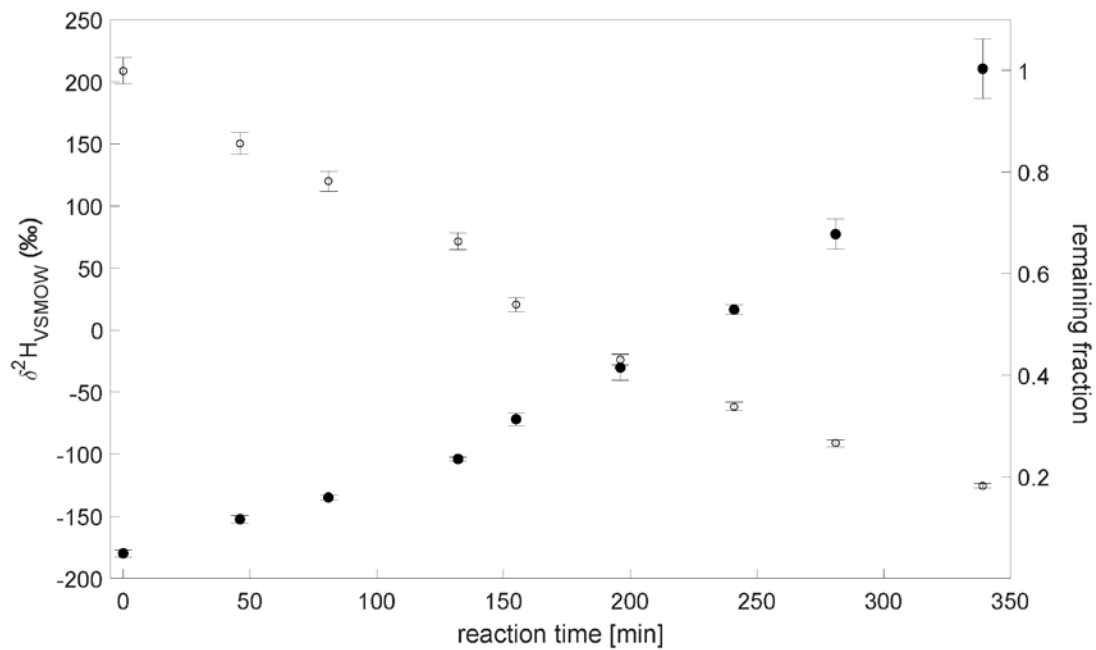
287

288

289 **Figure 4:** Reaction of CH<sub>4</sub> and OH. Initial mixing ratio of CH<sub>4</sub> was ~6 ppmv. More than 80%  
 290 of the CH<sub>4</sub> was degraded within 7 h. (a) Measured  $\delta^2\text{H}$  values of CH<sub>4</sub> versus residual fraction  
 291 of CH<sub>4</sub>. Error bars of  $\delta^2\text{H}$  values of CH<sub>4</sub> indicate the standard deviation (SD) of the mean of  
 292 three replicate measurements. Some error bars lie within the symbol. (b) Rayleigh plot  
 293 (equation 2). Error bars were calculated by error propagation including uncertainties in  $\delta^2\text{H}$   
 294 values of CH<sub>4</sub> and the remaining fraction. Dashed lines represent 95% confidence intervals of  
 295 the linear regressions (bold line).

296

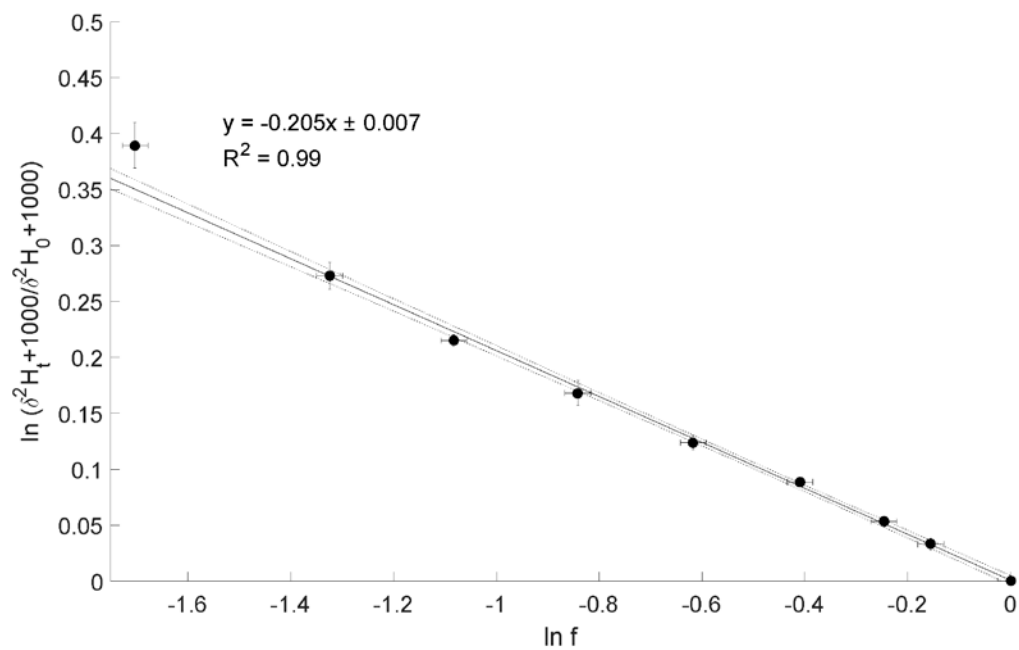
4a)



297

298

4b)



299

#### 300 4 Discussion

301 Chloromethane reacts with both hydroxyl and chlorine radicals in the atmosphere. The first  
302 degradation step of  $\text{CH}_3\text{Cl}$  in both reactions is the abstraction of a hydrogen atom to yield  
303  $\text{CH}_2\text{Cl}$  and  $\text{H}_2\text{O}$  or  $\text{HCl}$ , respectively (Spence et al., 1976; Khalil and Rasmussen, 1999). In

304 both reactions hydrogen is directly present in the reacting bond, and thus influenced by the  
305 so-called primary isotope effect (Elsner et al., 2005). Particularly for hydrogen these primary  
306 kinetic isotope effects are in general large as they involve a large change in relative mass of  
307 the atoms being abstracted. In the following we would like to discuss and compare our results  
308 with (i) previous work conducted by (Sellevåg et al., 2006), (ii) with OH degradation  
309 experiments of CH<sub>4</sub> and (iii) with the very recent report of biochemical degradation of CH<sub>3</sub>Cl  
310 in soils and plants (Jaeger et al., 2018b; Jaeger et al., 2018a).

311 Although our experimental results show relatively large hydrogen isotope fractionations with  
312  $\epsilon$  values of  $-264 \pm 45$  (mean result from three independent experiments  $\pm$  SD) and  $-280 \pm 11$   
313 ‰ (mean result from three replicate analytical measurements of the same sample  $\pm$  SD) for  
314 reaction of CH<sub>3</sub>Cl with OH and Cl radicals, respectively, they are smaller than the isotope  
315 fractionations previously measured and theoretically calculated by (Sellevåg et al., 2006)  
316 (Table 1). These researchers employed smog chamber experiments at 298 K and used FTIR  
317 measurements to determine the stable hydrogen isotope fractionation of CH<sub>3</sub>Cl and reported  $\epsilon$   
318 values of -410 and -420 ‰ for the reaction of CH<sub>3</sub>Cl with OH and Cl radicals, respectively.  
319 They also performed theoretical calculations of  $\epsilon$  for the reactions of CH<sub>2</sub>DCl with OH and  
320 Cl radicals and reported  $\epsilon$  values in the range of -330 to -430 and -540 to -590 ‰,  
321 respectively (Table 1). Whilst we do not know the reasons for the discrepancies in the  
322 experimental  $\epsilon$  values observed here and those reported by Sellevåg et al. (2006), we suggest  
323 that they may be due to different measurement techniques employed in each of the studies.  
324 For further discussion regarding differences of the experimental and analytical design and  
325 protocols of the two studies we would refer the reader to the Supplementary. However, we  
326 also conducted similar smog chamber experiments for the degradation of CH<sub>4</sub> with hydroxyl  
327 radicals (see methods section and Figure 4) and calculated an  $\epsilon$  value of  $-205 \pm 6$  ‰ for the  
328 reaction of CH<sub>4</sub> with OH radicals at a temperature of  $293 \pm 1$  K. In Table 1 we compare our  
329 results with those from a number of previous studies (Saueressig et al., 2001; Sellevåg et al.,  
330 2006; DeMore, 1993; Gierczak et al., 1997; Xiao et al., 1993), which were conducted at  
331 temperatures ranging from 277 to 298 K (Table 1). The  $\epsilon$  values for the reaction of CH<sub>4</sub> with  
332 OH radicals from all studies ranged from -145 to -294 ‰ with a mean value of  $-229 \pm 44$  ‰  
333 with the most negative  $\epsilon$  value of  $-294 \pm 18$  ‰ reported by Sellevåg and coworkers (2006).  
334 The  $\epsilon$  value found in this study ( $-205 \pm 6$  ‰) was in good agreement with previous  
335 experimentally reported values conducted at similar temperatures. This finding gave us

336 confidence that our experimental design and the measurements made using GC-IRMS were  
337 reliable.

338 Compared to primary isotope effects, changes in bonding are much smaller in the case of  
339 secondary isotope effects, where positions adjacent to the reacting bond are only slightly  
340 affected by the proximity to the reaction centre (Elsner et al., 2005; Kirsch, 1977). It was  
341 suggested that for the same element, secondary isotope effects are generally at least 1 order of  
342 magnitude smaller than primary isotope effects (Kirsch, 1977; Westaway, 1987; Merrigan et  
343 al., 1999).

344 We therefore compared our results from chemical degradation experiments with those from  
345 recently reported biochemical degradation experiments (Jaeger et al., 2018a; Jaeger et al.,  
346 2018b). So far, the only known pathway for biochemical consumption of CH<sub>3</sub>Cl is corrinoid-  
347 and tetrahydrofolate-dependent and is termed *cmu* (abbreviation for chloromethane  
348 utilization). This pathway was characterized in detail for the aerobic facultative  
349 methylotrophic strain *Methylobacterium extorquens* CM4 (Vannelli et al., 1999) and involves  
350 genes that were also detected in several other chloromethane-degrading strains (Schafer et al.,  
351 2007; Nadalig et al., 2013; Nadalig et al., 2011). During degradation of CH<sub>3</sub>Cl the methyl  
352 group is transferred to a corrinoid cofactor by the protein CmuA. In this case the carbon-  
353 chlorine bond of CH<sub>3</sub>Cl is broken and thus since the hydrogen atoms are adjacent to the  
354 reacting bond only a secondary isotope effect would be expected. Indeed, the first  $\epsilon$  values  
355 reported (Jaeger et al., 2018a; Jaeger et al., 2018b) for CH<sub>3</sub>Cl biodegradation by different  
356 soils and plants (ferns) are in the range of  $-50 \pm 13$  ‰ and  $-8 \pm 19$  ‰, respectively, and thus  
357 showing considerably smaller kinetic isotope effects than for chemical degradation of CH<sub>3</sub>Cl  
358 by OH and Cl radicals measured in either this study or reported by Sellevåg et al. (2006).

359

## 360 **5 Conclusions and future perspectives**

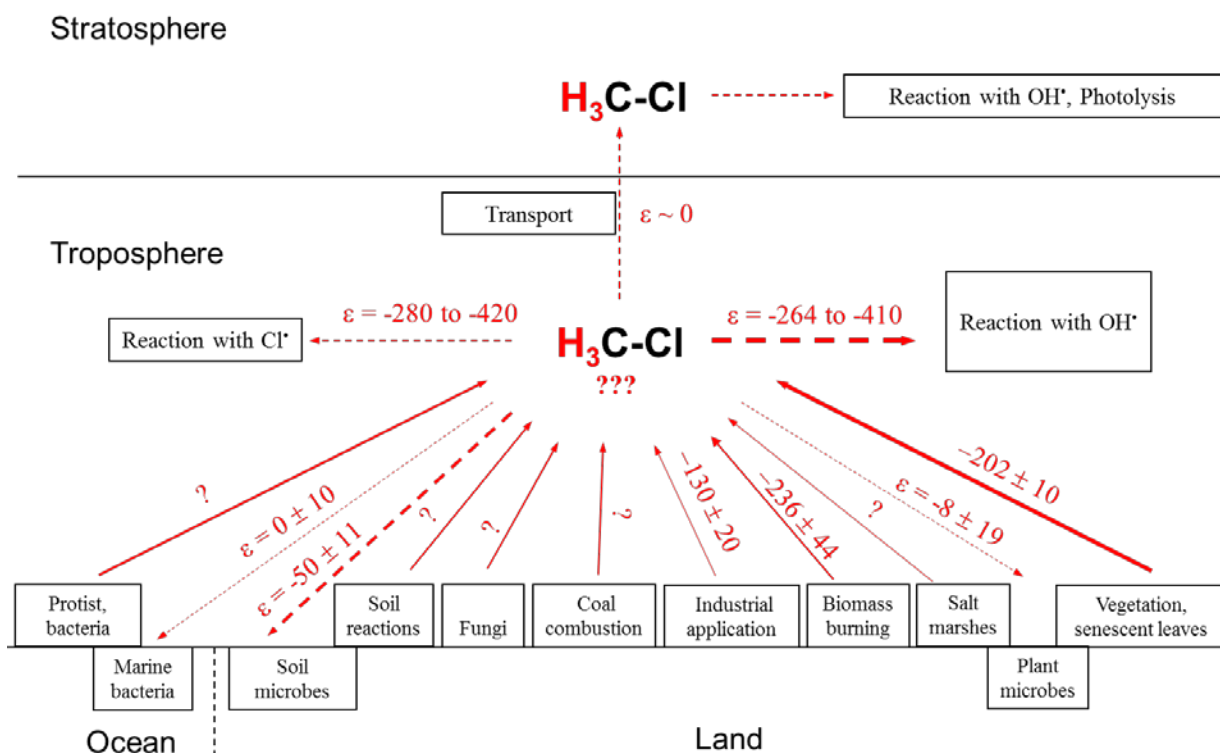
361 We have performed experiments to measure the hydrogen isotope fractionation of the  
362 remaining unreacted CH<sub>3</sub>Cl following its degradation by hydroxyl and chlorine radicals in a  
363 3.5 m<sup>3</sup> Teflon smog-chamber at  $293 \pm 1$  K.  $\delta^2$ H values of CH<sub>3</sub>Cl were measured using GC-  
364 IRMS. The calculated isotope fractionations of CH<sub>3</sub>Cl for the reactions with hydroxyl and  
365 with chlorine radicals were found to be smaller than either the experimentally measured (by  
366 FTIR) or theoretical values reported by Sellevåg et al. (2006). We also performed  
367 degradation experiments of CH<sub>4</sub> using the same smog-chamber facilities yielding an isotope

368 enrichment constant for the reaction of CH<sub>4</sub> with hydroxyl radicals of  $-205 \pm 6$  ‰ which is in  
 369 good agreement with previous reported results. Although stable hydrogen isotope  
 370 measurements of CH<sub>3</sub>Cl sources are still scarce, some recent studies have reported first data  
 371 on  $\delta^2\text{H}$  values of CH<sub>3</sub>Cl sources and  $\epsilon$  values on sinks (Greule et al., 2012; Jaeger et al.,  
 372 2018a; Jaeger et al., 2018b; Nadalig et al., 2014; Nadalig et al., 2013).

373 We have summarized all available information regarding  $\delta^2\text{H}$  values of environmental CH<sub>3</sub>Cl  
 374 sources and their estimated fluxes in Table 2. Furthermore, the strengths of known CH<sub>3</sub>Cl  
 375 sinks and their associated isotope enrichment constants are presented in Table 3. Eventually  
 376 Figure 5 displays the global CH<sub>3</sub>Cl budget showing the known hydrogen isotope signatures  
 377 of sources and isotope enrichment constants associated with sinks.

378 **Figure 5.** Scheme of major sources and sinks involved in the global CH<sub>3</sub>Cl cycle (modified  
 379 after Keppler et al., 2005) with known (experimentally determined) corresponding  $\delta^2\text{H}$  values  
 380 and isotope enrichment constants, respectively. Red straight and dashed lines of arrows  
 381 indicate sources and sinks of CH<sub>3</sub>Cl, respectively. Size/thickness of arrows indicate strength  
 382 of fluxes in the environment. Questions marks indicate where currently no data exist. All  
 383 values are given in ‰.

384



385

386

387 Our results suggest that stable hydrogen isotope measurements of both sources and sinks of  
388 CH<sub>3</sub>Cl and particularly the observed large kinetic isotope effect of the atmospheric CH<sub>3</sub>Cl  
389 sinks might strongly assist with the refinement of current models of the global atmospheric  
390 CH<sub>3</sub>Cl budget. In contrast to the large hydrogen fractionation of CH<sub>3</sub>Cl by chemical  
391 degradation of OH and Cl radicals, the isotope fractionation of CH<sub>3</sub>Cl biodegradation are in  
392 the range of an order of magnitude lower. This therefore holds the opportunity to improve our  
393 understanding of the global CH<sub>3</sub>Cl budget once the  $\delta^2\text{H}$  value of atmospheric CH<sub>3</sub>Cl has been  
394 measured. The stable hydrogen isotopic composition of tropospheric CH<sub>3</sub>Cl depends on the  
395 isotopic source signatures and the kinetic isotope effects of the sinks, primarily the reaction  
396 with OH and consumption by soils and potentially plants.

397 Several attempts at modelling the global CH<sub>3</sub>Cl budget using stable carbon isotope ratios  
398 have already been made (Harper et al., 2001; Harper et al., 2003; Thompson et al., 2002;  
399 Keppler et al., 2005; Saito and Yokouchi, 2008) but there are still major uncertainties  
400 regarding source and sink strengths as well as the respective stable isotope signatures.  
401 Therefore, we now suggest combining our knowledge of stable carbon and hydrogen isotopes  
402 of CH<sub>3</sub>Cl in the environment. Such a two dimensional (2D) stable isotope approach of  
403 hydrogen and carbon can be used to better understand the processes of CH<sub>3</sub>Cl biodegradation  
404 and formation. Furthermore, when this approach is combined with CH<sub>3</sub>Cl flux estimates it  
405 could help to better constrain the strength of CH<sub>3</sub>Cl sinks and sources within the global  
406 CH<sub>3</sub>Cl budget (Nadalig et al., 2014; Jaeger et al. 2018b)

407 We would highlight that currently no data is available for the  $\delta^2\text{H}$  value of atmospheric  
408 CH<sub>3</sub>Cl. Although it will be a massive analytical challenge to obtain this value, we strongly  
409 consider that it would likely lead to a better refined isotopic mass balance for atmospheric  
410 CH<sub>3</sub>Cl and thus to our better understanding of the global CH<sub>3</sub>Cl budget.

411

## 412 **Acknowledgements**

413 This study was supported by DFG (KE 884/8-1; KE 884/8-2, KE 884/10-1) and by the DFG  
414 research unit 763 'Natural Halogenation Processes in the Environment - Atmosphere and  
415 Soil' (KE 884/7-1, SCHO 286/7-2, ZE 792/5-2). We further acknowledge the German  
416 Federal Ministry of Education and Research (BMBF) for funding within SOPRAN 'Surface  
417 Ocean Processes in the Anthropocene (grants 03F0611E and 03F0662E). We thank John

418 Hamilton and Carl Brenninkmeijer for comments on an earlier version of the manuscript and  
419 Daniela Polag for statistical evaluation of the data.

420

## 421 **References**

422 Bleicher, S., Buxmann, J. C., Sander, R., Riedel, T. P., Thornton, J. A., Platt, U., and Zetzsch, C.: The  
423 influence of nitrogen oxides on the activation of bromide and chloride in salt aerosol, *Atmos. Chem.*  
424 *Phys. Discuss.*, 2014, 10135-10166, 10.5194/acpd-14-10135-2014, 2014.

425 Brenninkmeijer, C. A. M., Janssen, C., Kaiser, J., Röckmann, T., Rhee, T. S., and Assonov, S. S.:  
426 Isotope Effects in the Chemistry of Atmospheric Trace Compounds, *Chem. Rev.*, 103, 5125-5162,  
427 10.1021/cr020644k, 2003.

428 Carpenter, L. J., Reimann, S., Burkholder, J. B., Clerbaux, C., Hall, B., Hossaini, R., Laube, J., and  
429 Yvon-Lewis, S.: Chapter 1: Update on Ozone-Depleting Substances (ODSs) and Other Gases of  
430 Interest to the Montreal Protocol, in: *Scientific Assessment of Ozone Depletion, Global Ozone*  
431 *Research and Monitoring Project Report, World Meteorological Organization (WMO)*, 21-125, 2014.

432 Clark, I., and Fritz, P.: *Environmental isotopes in hydrogeology*, Lewis Publishers, New York, 328  
433 pp., 1997.

434 DeMore, W. B.: Rate constant ratio for the reaction of OH with CH<sub>3</sub>D and CH<sub>4</sub>., *J. Phys. Chem.*, 97,  
435 8564–8566, 1993.

436 Derendorp, L., Holzinger, R., Wishkerman, A., Keppler, F., and Rockmann, T.: Methyl chloride and  
437 C(2)-C(5) hydrocarbon emissions from dry leaf litter and their dependence on temperature, *Atmos.*  
438 *Environ.*, 45, 3112-3119, 10.1016/j.atmosenv.2011.03.016, 2011.

439 Elsner, M., Zwank, L., Hunkeler, D., and Schwarzenbach, R. P.: A new concept linking observable  
440 stable isotope fractionation to transformation pathways of organic pollutants, *Environ Sci Technol*,  
441 39, 6896-6916, 2005.

442 Gensch, I., Kiendler-Scharr, A., and Rudolph, J.: Isotope ratio studies of atmospheric organic  
443 compounds: Principles, methods, applications and potential, *International Journal of Mass*  
444 *Spectrometry*, 365-366, 206-221, <https://doi.org/10.1016/j.ijms.2014.02.004>, 2014.

445 Gierczak, T., Talukdar, R. K., Herndon, S. C., Vaghjiani, G. L., and Ravishankara, A. R.: Rate  
446 Coefficients for the Reactions of Hydroxyl Radicals with Methane and Deuterated Methanes, *The*  
447 *Journal of Physical Chemistry A*, 101, 3125-3134, 10.1021/jp963892r, 1997.

448 Gola, A. A., D'Anna, B., Feilberg, K. L., Sellevåg, S. R., Bache-Andreassen, L., and Nielsen, C. J.:  
449 Kinetic isotope effects in the gas phase reactions of OH and Cl with CH<sub>3</sub>Cl, CD<sub>3</sub>Cl, and (CH<sub>3</sub>Cl)-C-  
450 13, *Atmos. Chem. Phys.*, 5, 2395-2402, 2005.

451 Greule, M., Huber, S. G., and Keppler, F.: Stable hydrogen-isotope analysis of methyl chloride  
452 emitted from heated halophytic plants, *Atmos. Environ.*, 62, 584-592,  
453 10.1016/j.atmosenv.2012.09.007, 2012.

454 Hamilton, J. T. G., McRoberts, W. C., Keppler, F., Kalin, R. M., and Harper, D. B.: Chloride  
455 methylation by plant pectin: An efficient environmentally significant process, *Science*, 301, 206-209,  
456 2003.

457 Harper, D. B.: Halomethane from halide ion – a highly efficient fungal conversion of environmental  
458 significance, *Nature*, 315, 55-57, 1985.

459 Harper, D. B., Kalin, R. M., Hamilton, J. T. G., and Lamb, C.: Carbon isotope ratios for  
460 chloromethane of biological origin: Potential tool in determining biological emissions, *Environ. Sci.*  
461 *Technol.*, 35, 3616-3619, 2001.

462 Harper, D. B., Hamilton, J. T. G., Ducrocq, V., Kennedy, J. T., Downey, A., and Kalin, R. M.: The  
463 distinctive isotopic signature of plant-derived chloromethane: possible application in constraining the  
464 atmospheric chloromethane budget, *Chemosphere*, 52, 433-436, 2003.

465 Jaeger, N., Besaury, I., Kröber, E., Delort, A.-M., Greule, M., Lenhart, K., Nadalig, T., Vuilleumier,  
466 S., Amato, P., Kolb, S., Bringel, F., and Keppler, F.: Chloromethane degradation in soils - a combined  
467 microbial and two-dimensional stable isotope approach, *Journal of Environmental Quality*, 47, 254-  
468 262, 2018a.

469 Jaeger, N., Besaury, L., Röhling, A. N., Koch, F., Delort, A. M., Gasc, C., Greule, M., Kolb, S.,  
470 Nadalig, T., Peyret, P., Vuilleumier, S., Amato, P., Bringel, F., and Keppler, F.: Chloromethane  
471 formation and degradation in the fern phyllosphere, *Science of The Total Environment*, in press,  
472 2018b.

473 Keppler, F., Eiden, R., Niedan, V., Pracht, J., and Scholer, H. F.: Halocarbons produced by natural  
474 oxidation processes during degradation of organic matter, *Nature*, 403, 298-301, 2000.

475 Keppler, F., Harper, D. B., Rockmann, T., Moore, R. M., and Hamilton, J. T. G.: New insight into the  
476 atmospheric chloromethane budget gained using stable carbon isotope ratios, *Atmos. Chem. Phys.*, 5,  
477 2403-2411, 2005.

478 Keppler, F., Fischer, J., Sattler, T., Polag, D., Jaeger, N., Schöler, H. F., and Greule, M.:  
479 Chloromethane emissions in human breath, *Science of The Total Environment*, 605-606, 405-410,  
480 <https://doi.org/10.1016/j.scitotenv.2017.06.202>, 2017.

481 Khalil, M. A. K., Moore, R. M., Harper, D. B., Lobert, J. M., Erickson, D. J., Koropalov, V., Sturges,  
482 W. T., and Keene, W. C.: Natural emissions of chlorine-containing gases: Reactive Chlorine  
483 Emissions Inventory, *J. Geophys. Res.-Atmos.*, 104, 8333-8346, 1999.

484 Khalil, M. A. K., and Rasmussen, R. A.: Atmospheric methyl chloride, *Atmos. Environ.*, 33, 1305-  
485 1321, [https://doi.org/10.1016/S1352-2310\(98\)00234-9](https://doi.org/10.1016/S1352-2310(98)00234-9), 1999.

486 Kirsch, J. F.: in: *Isotope effects on enzyme-catalyzed reactions*, edited by: Cleland, W. W., O'Leary,  
487 M. H., and Northrop, D. B., University Park Press, Baltimore, London, Tokyo, 100-121, 1977.

488 Kolusu, S. R., Schlünzen, K. H., Grawe, D., and Seifert, R.: Chloromethane and dichloromethane in  
489 the tropical Atlantic Ocean, *Atmos. Environ.*, 150, 417-424, 2017.

490 Li, S., Park, M.-K., Jo, C. O., and Park, S.: Emission estimates of methyl chloride from industrial  
491 sources in China based on high frequency atmospheric observations, *Journal of Atmospheric*  
492 *Chemistry*, 1-17, [10.1007/s10874-016-9354-4](https://doi.org/10.1007/s10874-016-9354-4), 2016.

493 McAnulla, C., McDonald, I. R., and Murrell, J. C.: Methyl chloride utilising bacteria are ubiquitous in  
494 the natural environment, *FEMS Microbiology Letters*, 201, 151-155, [10.1111/j.1574-  
495 6968.2001.tb10749.x](https://doi.org/10.1111/j.1574-6968.2001.tb10749.x), 2001.

496 Merrigan, S. R., Le Gloahec, V. N., Smith, J. A., Barton, D. H. R., and Singleton, D. A.: Separation of  
497 the primary and secondary kinetic isotope effects at a reactive center using starting material  
498 reactivities. Application to the FeCl<sub>3</sub>-Catalyzed oxidation of C-H bonds with *tert*-butyl  
499 hydroperoxide, *Tetrahedron Letters*, 40, 3847-3850, [https://doi.org/10.1016/S0040-4039\(99\)00637-1](https://doi.org/10.1016/S0040-4039(99)00637-1),  
500 1999.

501 Miller, L. G., Kalin, R. M., McCauley, S. E., Hamilton, J. T. G., Harper, D. B., Millet, D. B.,  
502 Oremland, R. S., and Goldstein, A. H.: Large carbon isotope fractionation associated with oxidation  
503 of methyl halides by methylotrophic bacteria, *Proc. Natl. Acad. Sci. U. S. A.*, 98, 5833-5837, 2001.

504 Miller, L. G., Warner, K. L., Baesman, S. M., Oremland, R. S., McDonald, I. R., Radajewski, S., and  
505 Murrell, J. C.: Degradation of methyl bromide and methyl chloride in soil microcosms: Use of stable  
506 C isotope fractionation and stable isotope probing to identify reactions and the responsible  
507 microorganisms, *Geochim. Cosmochim. Acta*, 68, 3271-3283, 2004.

508 Montzka, S. A., and Fraser, P.: Controlled substances and other source gases, Chapter 1 in *Scientific*  
509 *Assessment of Ozone Depletion: 2002*, World Meteorological Organization, Geneva, 2003.

510 Moore, R. M., Groszko, W., and Niven, S. J.: Ocean-atmosphere exchange of methyl chloride:  
511 Results from NW Atlantic and Pacific Ocean studies, *J. Geophys. Res.-Oceans*, 101, 28529-28538,  
512 10.1029/96jc02915, 1996.

513 Nadalig, T., Farhan Ul Haque, M., Roselli, S., Schaller, H., Bringel, F., and Vuilleumier, S.: Detection  
514 and isolation of chloromethane-degrading bacteria from the *Arabidopsis thaliana* phyllosphere, and  
515 characterization of chloromethane utilization genes, *FEMS Microbiology Ecology*, 77, 438-448,  
516 10.1111/j.1574-6941.2011.01125.x, 2011.

517 Nadalig, T., Greule, M., Bringel, F., Vuilleumier, S., and Keppler, F.: Hydrogen and carbon isotope  
518 fractionation during degradation of chloromethane by methylotrophic bacteria, *MicrobiologyOpen*, 2,  
519 893-900, 10.1002/mbo3.124, 2013.

520 Nadalig, T., Greule, M., Bringel, F., Keppler, F., and Vuilleumier, S.: Probing the diversity of  
521 chloromethane-degrading bacteria by comparative genomics and isotopic fractionation, *Frontiers in*  
522 *Microbiology*, 5, 523, 10.3389/fmicb.2014.00523, 2014.

523 Redeker, K. R., Wang, N.-Y., Low, J. C., McMillan, A., Tyler, S. C., and Cicerone, R. J.: Emissions  
524 of Methyl Halides and Methane from Rice Paddies, *Science*, 290, 966-969,  
525 10.1126/science.290.5493.966, 2000.

526 Rhew, R. C., Miller, B. R., and Weiss, R. F.: Natural methyl bromide and methyl chloride emissions  
527 from coastal salt marshes, *Nature*, 403, 292-295, 10.1038/35002043, 2000.

528 Rhew, R. C., Aydin, M., and Saltzman, E. S.: Measuring terrestrial fluxes of methyl chloride and  
529 methyl bromide using a stable isotope tracer technique, *Geophys. Res. Lett.*, 30, 5, 2003.

530 Saito, T., and Yokouchi, Y.: Stable carbon isotope ratio of methyl chloride emitted from glasshouse-  
531 grown tropical plants and its implication for the global methyl chloride budget, *Geophys. Res. Lett.*,  
532 35, 2008.

533 Saueressig, G., Crowley, J. N., Bergamaschi, P., Brühl, C., Brenninkmeijer, C. A. M., and Fischer, H.:  
534 Carbon 13 and D kinetic isotope effects in the reactions of CH<sub>4</sub> with O(1D) and OH: New laboratory  
535 measurements and their implications for the isotopic composition of stratospheric methane, *Journal of*  
536 *Geophysical Research: Atmospheres*, 106, 23127-23138, 10.1029/2000JD000120, 2001.

537 Schafer, H., Miller, L. G., Oremland, R. S., and Murrell, J. C.: Bacterial cycling of methyl halides, in:  
538 *Advances in Applied Microbiology*, *Advances in Applied Microbiology*, 307-346, 2007.

539 Sellevåg, S. R., Nyman, G., and Nielsen, C. J.: Study of the Carbon-13 and Deuterium Kinetic Isotope  
540 Effects in the Cl and OH Reactions of CH<sub>4</sub> and CH<sub>3</sub>Cl, *The Journal of Physical Chemistry A*, 110,  
541 141-152, 10.1021/jp0549778, 2006.

542 Spence, J. W., Hanst, P. L., and Gay, B. W.: Atmospheric Oxidation of Methyl Chloride Methylene  
543 Chloride, and Chloroform, *Journal of the Air Pollution Control Association*, 26, 994-996,  
544 10.1080/00022470.1976.10470354, 1976.

545 Thompson, A. E., Anderson, R. S., Rudolph, J., and Huang, L.: Stable carbon isotope signatures of  
546 background tropospheric chloromethane and CFC113, *Biogeochemistry*, 60, 191-211, 2002.

547 Umezawa, T., Baker, A. K., Brenninkmeijer, C. A. M., Zahn, A., Oram, D. E., and van Velthoven, P.  
548 F. J.: Methyl chloride as a tracer of tropical tropospheric air in the lowermost stratosphere inferred  
549 from IAGOS-CARIBIC passenger aircraft measurements, *Journal of Geophysical Research:*  
550 *Atmospheres*, 120, 12,313-312,326, 10.1002/2015JD023729, 2015.

551 Urey, H. C.: Oxygen Isotopes in Nature and in the Laboratory, *Science*, 108, 489-496,  
552 10.1126/science.108.2810.489, 1948.

553 Vannelli, T., Messmer, M., Studer, A., Vuilleumier, S., and Leisinger, T.: A corrinoid-dependent  
554 catabolic pathway for growth of a *Methylobacterium* strain with chloromethane, *Proceedings of the*  
555 *National Academy of Sciences*, 96, 4615-4620, 10.1073/pnas.96.8.4615, 1999.

- 556 Westaway, K. C.: in: *Isotopes in organic chemistry*, vol. 8: Secondary and solvent isotope effects,  
557 edited by: Buncl, E., and Lee, C. C., Elsevier, Amsterdam, Oxford, New York, Tokyo, 275-392,  
558 1987.
- 559 Williams, J., Wang, N.-Y., Cicerone, R. J., Yagi, K., Kurihara, M., and Terada, F.: Atmospheric  
560 methyl halides and dimethyl sulfide from cattle, *Glob. Biogeochem. Cycle*, 13, 485-491,  
561 10.1029/1998GB900010, 1999.
- 562 Wittmer, J., Bleicher, S., and Zetzsch, C.: Iron(III)-induced activation of chloride and bromide from  
563 modeled salt pans, *The journal of physical chemistry. A*, 119, 4373-4385, 10.1021/jp508006s, 2015.
- 564 WMO: *Scientific Assessment of Ozone Depletion: 2010*, Global Ozone Research and Monitoring  
565 Project-Report No. 52, 516 pp., Geneva, Switzerland, 2011.
- 566 Xiao, Y., Tanaka, N., and Lasaga, A.: An evaluation of hydrogen kinetic isotope effect in the reaction  
567 of CH<sub>4</sub> with OH free radical (abstract). In: *Eos Trans. AGU*, 74, Spring Meet. Suppl., 71., 1993.
- 568 Yokouchi, Y., Ikeda, M., Inuzuka, Y., and Yukawa, T.: Strong emission of methyl chloride from  
569 tropical plants, *Nature*, 416, 163-165, 2002.
- 570 Yokouchi, Y., Saito, T., Ishigaki, C., and Aramoto, M.: Identification of methyl chloride-emitting  
571 plants and atmospheric measurements on a subtropical island, *Chemosphere*, 69, 549-553, 2007.  
572
- 573
- 574

575 Table 1: Reported hydrogen isotope enrichment constants for the reaction of CH<sub>3</sub>Cl with OH  
 576 radicals and with Cl atoms and the reaction of CH<sub>4</sub> with OH radicals.

Reaction	$\epsilon$ / ‰	Method and remarks	Reference
CH <sub>3</sub> Cl + OH	-264 ± 45	experimental: 3.5 m <sup>3</sup> smog-chamber at 293 ± 1 K; Exp. 1 to 3, this study IRMS	
CH <sub>3</sub> Cl + OH	-410 ± 50	experimental: smog-chamber, long-path FTIR spectroscopy relative to CH <sub>3</sub> Cl at 298 ± 2 K	Sellevåg et al. 2006
CH <sub>3</sub> Cl + OH	-330 to -430	theoretical calculations	Sellevåg et al. 2006
CH <sub>3</sub> Cl + Cl	-280 ± 11	experimental: 3.5 m <sup>3</sup> smog-chamber at 293 ± 1 K; Exp. 4, this study IRMS	
CH <sub>3</sub> Cl + Cl	-420 ± 40	experimental: smog-chamber, long-path FTIR spectroscopy relative to CH <sub>3</sub> Cl at 298 ± 2 K	Sellevåg et al. 2006
CH <sub>3</sub> Cl + Cl	-540 to -590	theoretical calculations	Sellevåg et al. 2006
CH <sub>4</sub> + OH	-205 ± 6	experimental: 3.5 m <sup>3</sup> smog-chamber at 293 ± 1 K; Exp. 5, this study IRMS	
CH <sub>4</sub> + OH	-227 ± 11	experimental: at 296 K, IRMS and tunable diode laser absorption spectroscopy	Saueressig et al. 2001
CH <sub>4</sub> + OH	-231 ± 45	experimental: at 277 K	Gierczak et al., 1997
CH <sub>4</sub> + OH	-251 ± 10	ab initio at 298 K	Xiao et al., 1993
CH <sub>4</sub> + OH	-145 ± 30	experimental: at 298 K	DeMore et al., 1993
CH <sub>4</sub> + OH	-294 ± 18	experimental: smog-chamber, long-path FTIR spectroscopy relative to CH <sub>3</sub> Cl at 298 ± 2 K	Sellevåg et al. 2006
CH <sub>4</sub> + OH	-60 to -270	theoretical at 298 K	Sellevåg et al. 2006

**Table 2.** Known sources and strengths of tropospheric CH<sub>3</sub>Cl and corresponding δ<sup>2</sup>H values.

Sources	Source (best estimate) <sup>a</sup> (Gg yr <sup>-1</sup> )	Source (full range) <sup>a</sup> (Gg yr <sup>-1</sup> )	Mean δ <sup>2</sup> H value ‰ vs VSMOV	Uncertainty δ <sup>2</sup> H value ± ‰
Open field biomass burning	355	142 to 569	-236 <sup>b</sup>	44
Biomass burning indoor	113	56 to 169	-236 <sup>b</sup>	44
Tropical and subtropical plants	2040	1430 to 2650	-202 <sup>c</sup>	10
Fungi	145	128 to 162	?	
Salt marshes	85	1.1 to 170	?	
Coal combustion	162	29 to 295	?	
Industrial chemical production <sup>d</sup>	363	278 to 448	-130 <sup>e</sup>	20
Oceans	700	510 to 910	?	
Others <sup>f</sup>	~58	27 to 86	?	
Total sources	3658 (4021)	2601 to 5459		

<sup>a</sup> Values for source (best estimate) and source (full range) were taken from Carpenter and Reimann (2014), except for emissions associated with chemical production by the industry which are from Li et al. (2016). Value shown for total sources in brackets includes chemical production by the industry.

<sup>b</sup> Greule et al. 2012; please note that all values provided for CH<sub>3</sub>Cl released from dried plants at elevated temperatures have been corrected by -23 ‰ due to recalibration of the reference gas.

<sup>c</sup> Jaeger et al. (2018b)

<sup>d</sup> Li et al. (2016)

<sup>e</sup> taken from Greule et al. (2012), Nadalig et al. (2013) and Jaeger et al. (2018a & 2018b); please note that values provided by Greule et al. (2012) and Nadalig et al. (2013) for CH<sub>3</sub>Cl from sources of the chemical industry have been corrected by -23 ‰ due to recalibration of the reference gas

<sup>f</sup> including mangroves, wetlands, rice paddies and shrublands

? denotes that no value has been provided

**Table 3.** Known sinks of tropospheric CH<sub>3</sub>Cl and the mean isotope enrichment constant  $\epsilon$  reported for each.

Sinks	Sink (best estimate) <sup>a</sup> (Gg yr <sup>-1</sup> )	Sink (full range) <sup>a</sup> (Gg yr <sup>-1</sup> )	Isotope enrichment constant	Uncertainty $\epsilon$
			$\epsilon$ / ‰	$\pm$ ‰
Reaction with OH in troposphere	2832	2470 to 3420	-264 <sup>b</sup> -410 <sup>c</sup>	45 <sup>b</sup> 50 <sup>c</sup>
Loss to stratosphere	146	?	0 <sup>d</sup>	?
Reaction with Cl in marine boundary layer	370 <sup>d</sup>	180 to 550 <sup>d</sup>	-280 <sup>b</sup> -420 <sup>c</sup>	11 <sup>b</sup> 40 <sup>c</sup>
Microbial degradation in soil	1058	664 to 1482	-50 <sup>e</sup>	13 <sup>e</sup>
Loss in ocean	370	296 to 445	0 <sup>f</sup>	10 <sup>f</sup>
Microbial degradation in plants <sup>g</sup>	?	?	-8 <sup>g</sup>	19 <sup>g</sup>
Total sinks	4406 (4776)			

<sup>a</sup> Values for sink strength (best estimate and full range) were taken from Carpenter and Reimann (2014), except for the value of the reaction with Cl-radicals in marine boundary layer and for total sinks shown in brackets which includes the potential sink strength by Cl-radicals in marine boundary layer (Montzka and Fraser, 2003).

<sup>b</sup> this study, mean value of three experiments

<sup>c</sup> Sellevåg et al. (2006)

<sup>d</sup> Thompson et al. (2002) and discussion in this manuscript

<sup>e</sup> Jaeger et al. (2018a)

<sup>f</sup> Nadalig et al. (2014)

<sup>g</sup> Jaeger et al. (2018b)

? denotes that no value has been provided